Theoretical prediction on the structural, electronic, and polarization properties of tetragonal Bi_2ZnTiO_6

Hai Wang,[1,a] Haitao Huang,[1] Wei Lu,[1] Helen L. W. Chan,[1] Biao Wang,[2] and C. H. Woo[3]
[1]*Department of Applied Physics and Materials Research Center, The Hong Kong Polytechnic University, Hong Kong, China*
[2]*School of Physics and Engineering, Sun Yat-sen University, Guangzhou 510275, China*
[3]*Department of Electronic and Information Engineering, The Hong Kong Polytechnic University, Hong Kong, China*

(Received 30 September 2008; accepted 17 January 2009; published online 12 March 2009)

We present first-principles investigations on the structural, electronic, and polarization properties of Bi_2ZnTiO_6 using density-functional theory within the generalized gradient approximation. The theoretical structure we obtained confirms the extra large tetragonality observed by experiment. The materials exhibit a semiconductor behavior with an indirect band gap determined by the occupied O $2p$ and unoccupied Bi $6p$ states. There are strong hybridization effects between Bi–O ions, as well as Ti–O and Zn–O ones. The resulting covalent bondings, having a $PbTiO_3$-type two-dimensional character, strengthen each other and favor the coupling between the tetragonal distortion of unit cell and the off-center displacement of A and B-site cations and O anions due to the existence of Zn, and result in the large tetragonality of this compound. Berry-phase calculation gives the polarization as high as 122 $\mu C/cm^2$. © *2009 American Institute of Physics*. [DOI: 10.1063/1.3086628]

I. INTRODUCTION

Perovskite $BiMO_3$ compound with a ABO_3 structure shows a versatility in physical properties which depend on the type of M ions. When M is a magnetic element, such as Fe and Mn, the material is multiferroic.[1–3] When M is nonmagnetic, such as Sc, it is a high-temperature piezoelectric when it forms a solid solution with $PbTiO_3$ (PT).[4–10] Recently, $BiMO_3$ has been theoretically predicted to be a promising lead-free ferroelectric, piezoelectric, or multiferroic material.[11,12] Unfortunately, most of the $BiMO_3$ compounds are unstable, except for $BiFeO_3$ and $BiMnO_3$. Therefore, many efforts have been put into the synthesis of $BiMO_3$ using high-temperature high-pressure techniques[13–16] or into the searching of the more stable structure by forming the B-site complex $BiMM'O_3$ compounds such as Bi_2NiTiO_6,[17] Bi_2MnNiO_6,[18] and Bi_2MgTiO_6.[19] While most of these compounds possess $GdFeO_3$-type distorted perovskite structure, Bi_2ZnTiO_6 (BZT) synthesized under high pressure shows a tetragonal structure with a special high tetragonality $c/a = 1.211$ among Pb- or Bi-based perovskite materials.[20] The large tetragonality of BZT was speculated to result from the coupled distortion of A- and B-site cations due to the special coordination geometry. It is well known that the tetragonality is related to the polarization,[21] piezoelectricity,[22] and pyroelectricity.[20] Hence, BZT with large tetragonality should be a promising candidate for multifunctional materials. Thanks to the large tetragonality of BZT, its solid solutions with other perovskite materials are promising high T_c ferroelectrics.[23] In addition, BZT itself is a potential pyroelectric with excellent properties for technical applications.

In fact, it is difficult to grow a BZT single crystal for studying the origin of tetragonality. To the best of our knowledge, there is so far no theoretical study on the origin of the large tetragonality in this compound. In this work, we have performed a series of first-principles density-functional calculations on the structural and electronic properties of BZT to examine the origin of its large tetragonality.

II. COMPUTATION METHOD

The calculations were performed using the accurate full-potential linear augmented plane-wave (FLAPW) method as implemented in WIEN2k code.[24] The Perdew–Burke–Ernzerhof generalized gradient approximation (GGA) was used for the exchange correlation potentials.[25] The semirelativistic approximation effects were employed in the calculation for the valence states, while the core levels were treated fully relativistically. A matrix size (convergence) parameter $R_{MT}K_{MAX}=8$ was used, where R_{MT} is the smallest atomic radius and K_{MAX} is the plane-wave cutoff. The muffin-tin radii of Bi, Zn, Ti, and O are 2.5, 2.1, 1.65, and 1.55 a.u., respectively. The Brillouin zone was sampled by $10\times10\times5$ k-point mesh. Experimentally, no ordering of the Zn and Ti cations on the B-site is observed in BZT. In this work, as shown in Fig. 1, we employed a smallest $1a\times1a\times2c$ supercell (artificial superlattice structure) to model BZT, where the experimental lattice constants of a and c are used as starting structure parameters. Each supercell contains ten atoms, where the B-site Zn and Ti ions are ordered along the [001] direction. To obtain the theoretical equilibrium structure for BZT, both the lattice constants (a and c) and the atomic positions were optimized within the framework of a tetragonal symmetry (space group $P4mm$). The density of states (DOS) is computed by the tetrahedron method;[26] the convergence on the k-point mesh was also examined.

In order to confirm the ground-state structure obtained

[a]Electronic mail: aphhuang@polyu.edu.hk.

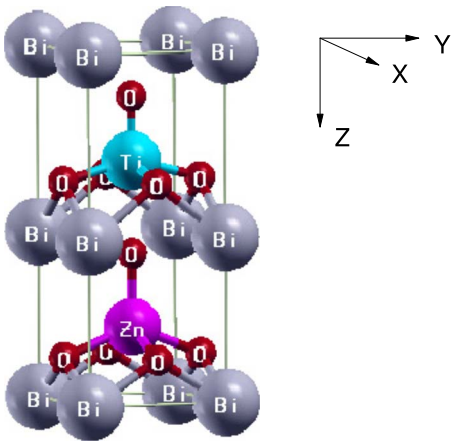

FIG. 1. (Color online) Schematic illustration of the crystal structure of Bi_2ZnTiO_6 with space group *P*4*mm*.

using FLAPW method, we also performed corresponding calculations employing another extensively used code, Vienna *ab initio* simulation package (VASP),[27] using the GGA on the basis of the projector augmented wave (PAW) method.[28] The plane-wave cutoff energy was set to 450 eV. These calculations were performed with a $10\times10\times5$ Monkhorst–Pack *k*-point mesh. Note that, except as otherwise indicated, the conditions used for VASP calculations are the same as that for WIEN2k. The electric polarization was calculated using the modern polarization theory.[29,30] We have used very large basis set with 600 eV for the plane-wave cutoff. For the *k*-space integration in the Berry-phase calculations, a uniform $16\times16\times8$ *k*-point mesh was found to be adequate.

III. RESULTS AND DISCUSSION

A. Ground-state structure

To examine the effectivity of supercell model of BZT used here, we first performed calculations using the experimental tetragonality c/a (1.211). The experimental and calculated structure parameters, total energy, and relaxed fractional atomic coordinates are listed in Table I and II, respectively. When the tetragonality c/a was set to the experimental value of 1.211, the calculated lattice parameters (a and c) are about 1% larger than the experimental values. This is very precise for density-functional theory (DFT) within GGA. The experimental and calculated bond lengths are given in Table III. It is noted that the experimental Ti–O and Zn–O bond lengths are the averaged values without differentiation between them. In fact, they should be different due to the difference in chemistry between Ti and Zn, that is, one basically has an unfilled *d* shell and the other a filled *d* shell (see Fig. 5). Our results are off by 10%–15% with the largest difference of 0.71 Å from the experimental results. They are still reasonable since the experimental values could not tell the difference between Ti–O and Zn–O bond lengths.

TABLE I. Experimental and calculated lattice parameters a, c (Å), equilibrium volume V (Å^3), and the polarization P (μC/cm^2) of BZT with different tetragonality c/a. In order to compare the stability, the energy difference ΔE (meV) are also given.

	a	c	c/a	V	P [a]	ΔE
Expt.[b]	3.822	4.628	1.211			
Calc.[c]	3.856	4.670	1.211	69.4		0
Calc.[d]	3.828	4.788	1.251	70.1		−66
Calc.[d]	3.791	4.940	1.311	71.2		−104
Calc.[e]	3.856	4.670	1.211		113	0
Calc.[f]	3.828	4.788	1.251		117	−67
Calc.[f]	3.791	4.940	1.311		122	−109

[a]This work. Berry-phase calculations using VASP.
[b]Reference 20.
[c]This work, WIEN2k-GGA. Its total energy as reference.
[d]This work, WIEN2k-GGA.
[e]This work, VASP-GGA-PAW. Its total energy as reference.
[f]This work, VASP-GGA-PAW.

TABLE II. Calculated atomic internal fractional coordinates of BZT from WIEN2k (upper part) and VASP (lower part) calculations.

c/a	All	1.211	1.251	1.311
Atom	x,y,z-δz	δz	δz	δz
Bi1	0.0,0.0,0.00	0.000	0.000	0.000
Ti	0.5,0.5,0.25	0.071	0.072	0.070
O1	0.5,0.5,0.00	0.138	0.144	0.148
O2	0.5,0.0,0.25	0.124	0.129	0.130
O3	0.0,0.5,0.25	0.124	0.129	0.130
Bi2	0.0,0.0,0.50	0.030	0.032	0.031
Zn	0.5,0.5,0.75	0.043	0.044	0.044
O4	0.5,0.5,0.50	0.085	0.090	0.095
O5	0.5,0.0,0.75	0.124	0.127	0.130
O6	0.0,0.5,0.75	0.124	0.127	0.130
Bi1	0.0,0.0,0.00	0.000	0.000	0.000
Ti	0.5,0.5,0.25	0.069	0.069	0.071
O1	0.5,0.5,0.00	0.135	0.140	0.149
O2	0.5,0.0,0.25	0.123	0.126	0.132
O3	0.0,0.5,0.25	0.123	0.126	0.132
Bi2	0.0,0.0,0.50	0.029	0.030	0.033
Zn	0.5,0.5,0.75	0.042	0.043	0.044
O4	0.5,0.5,0.50	0.083	0.088	0.097
O5	0.5,0.0,0.75	0.124	0.126	0.130
O6	0.0,0.5,0.75	0.124	0.126	0.130

TABLE III. Experimental and calculated bond lengths and the corresponding difference Δ(Calc−Expt) (Å) in the BZT. It is note that the obtainable experimental Ti–O and Zn–O bond lengths are the average values without the differentiation between Ti and Zn.

Bond	Expt.[a]	Calc.[b]	Δ [b]	Calc.[c]	Δ^c	$\Delta^c-\Delta^b$
Bi–O	2.385	2.258	−0.127	2.241	−0.144	−0.017
		2.417	+0.032	2.416	+0.031	−0.001
Bi–O	2.833	2.773	−0.060	2.756	−0.077	−0.017
Bi–O	3.728	3.015	−0.713	3.060	−0.668	−0.009
Ti–O	1.770	1.709	−0.061	1.706	−0.064	−0.003
Ti–O	1.997	1.992	−0.005	1.990	−0.007	−0.002
Ti–O	2.860	2.464	−0.396	2.741	−0.119	+0.277
Zn–O	1.770	1.948	+0.178	1.970	+0.200	+0.022
Zn–O	1.997	2.071	+0.074	2.078	+0.081	+0.007
Zn–O	2.860	3.218	+0.358	3.523	+0.663	+0.305

[a]Reference 20, tetragonality c/a 1.211.
[b]This work, tetragonality c/a=1.211 using WIEN2k-GGA.
[c]This work, tetragonality c/a=1.311 using WIEN2k-GGA.

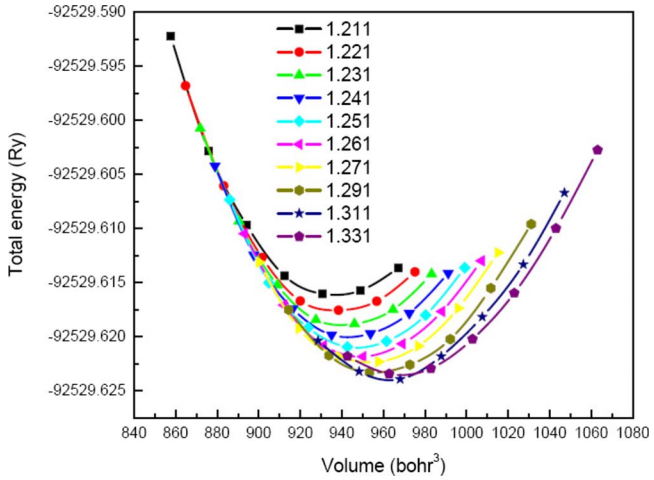

FIG. 2. (Color online) Calculated total energy as a function of volume in Bi_2ZnTiO_6 with different tetragonality.

Our calculations predict unequal Zn–O and Ti–O bond lengths. Similar results have also been reported in lead zirconate titanate $[PbZr_xTi_{1-x}O_3$ (PZT)] system due to the differences in ionic size of the metal cations.[31] This is consistent with the experimental Raman spectroscopy study showing the broadening of the (Zn,Ti)–O stretching and bending modes as compared to the corresponding Ti–O modes in $PbTiO_3$.[20] This means that the theoretical supercell method is effective to describe the local structural distortion of BZT. Those structural distortions may include the tetragonal distortion of the unit cell and the off-center displacements of all ions. The large off-center displacements of *B* site cation and surrounding O anions make the *B*-centered oxygen octahedra change to square based pyramids, as suggested by experiment.[20] Due to the difference in size of Zn and Ti ions, the bond of Ti–O should be different from that of Zn–O bond. The length of *c* of the cell containing Ti ion (equal to the distance of two Bi ions) is 4.95 Å, about 0.58 Å longer than that of the cell containing Zn (4.37 Å). This suggests that Bi ion also has an off-center displacement along *c* axis, which may be dependent on the B–O bond length. It is noted that the Ti–O bond length in BZT is very short as compared to that in a typical ferroelectric $Bi_4Ti_3O_{12}$,[32] indicating a much stronger covalent bonding of the Ti–O bonds in BZT.

To obtain the ground-state structure, full structure optimization was performed. During the structural optimization, it is found that the total energy of BZT can be decreased by either decreasing the lattice parameter *a* or increasing the tetragonality *c*/*a*. To determine the theoretical equilibrium structure, therefore, a series of calculations with varying lattice parameter *a* (about from 3.74 to 3.90 Å) and tetragonality *c*/*a* (from 1.211 to 1.331) were performed, where the fractional atomic coordinates are relaxed. The results are shown in Fig. 2. For a given tetragonality *c*/*a*, the total energy of BZT has a local minimum, corresponding to a equilibrium volume. As the tetragonality increases, the equilibrium volume of system increases while the corresponding total energy reduces until the global minimum is reached. The increase in equilibrium volume corresponds to a decrease in pressure, which results in an increase in tetragonality. The same phenomenon of the reduced tetragonality under higher pressure has been reported in $PbTiO_3$ (Ref. 33) and PZT system.[34–36]

The most energetically favorable lattice parameters calculated for Bi_2ZnTiO_6 are $a=3.791$ and $c=4.940$ Å, about 1% less and 7% more than the experimental results, respectively. The corresponding theoretical tetragonality is $c/a=1.311$, 8% larger than the experimental value. This is a surprisingly large tetragonality. To confirm the results obtained from WIEN2k calculations, VASP code using PAW potential was used to calculate fractional atomic coordinates with fixed lattice parameters *a* and *c* obtained from FLAPW method. The results are shown in Tables I and II. It is evident that both the total energy and the fractional atomic coordinates agree well with the FLAPW calculations, indicating that the calculated large tetragonality is reasonable. Our results show that the equilibrium volume is larger than the high-pressure experimental value, since our calculations were performed at zero temperature and zero pressure; and the larger tetragonality which is consistent with the fact that the tetragonality can be reduced by hydrostatic pressure. Here, we used DFT VASP method to confirm our FLAPW results. Further study on *B*-site order/disorder can be performed using VASP code, which is very useful for large size systems.

The structural optimization shows that the off-center displacement of an ion can reduce the total energy of the system until an equilibrium value is reached. As can be seen from Table II, when the tetragonality increases from 1.211 to 1.311, the change in fractional atomic coordinates is small. The last column of Table III shows that the bond lengths of Bi–O, Zn–O, and Ti–O are basically unchanged, except that the longest bond lengths of Ti–O and Zn–O are increased about 0.3 Å. This indicates strong coupling between the tetragonal distortion of the unit cell and internal atomic off-center displacement. As the tetragonality increases, internal atom distortions take place in order to keep the change of bond length as small as possible (Table III). In this case, since the total energy of system is reduce, this internal atomic distortion is energetically favorable and has a intrinsic strong coupling with tetragonal distortion of the unit cell. So, we guess that the bonding environment of BZT with increasing tetragonality maybe does not vary too much. The material shows a "self-adapting" character. This phenomenon might be of particular importance for the understanding of its physical origin and for developing new type of high-performance lead-free piezoelectric materials.

B. Electronic properties

1. Band structure

To understand the origin of large tetragonality and chemical bonding character, we performed electric structure calculation for BZTs with different tetragonalities $c/a=1.211$ and 1.311. Figure 3 shows the band structure of BZT along the high-symmetry directions in the first Brillouin zone. Fermi level is located at 0 eV. It is evident that the band structures of two BZTs with different tetragonalities are substantially similar. This is consistent with the bonding

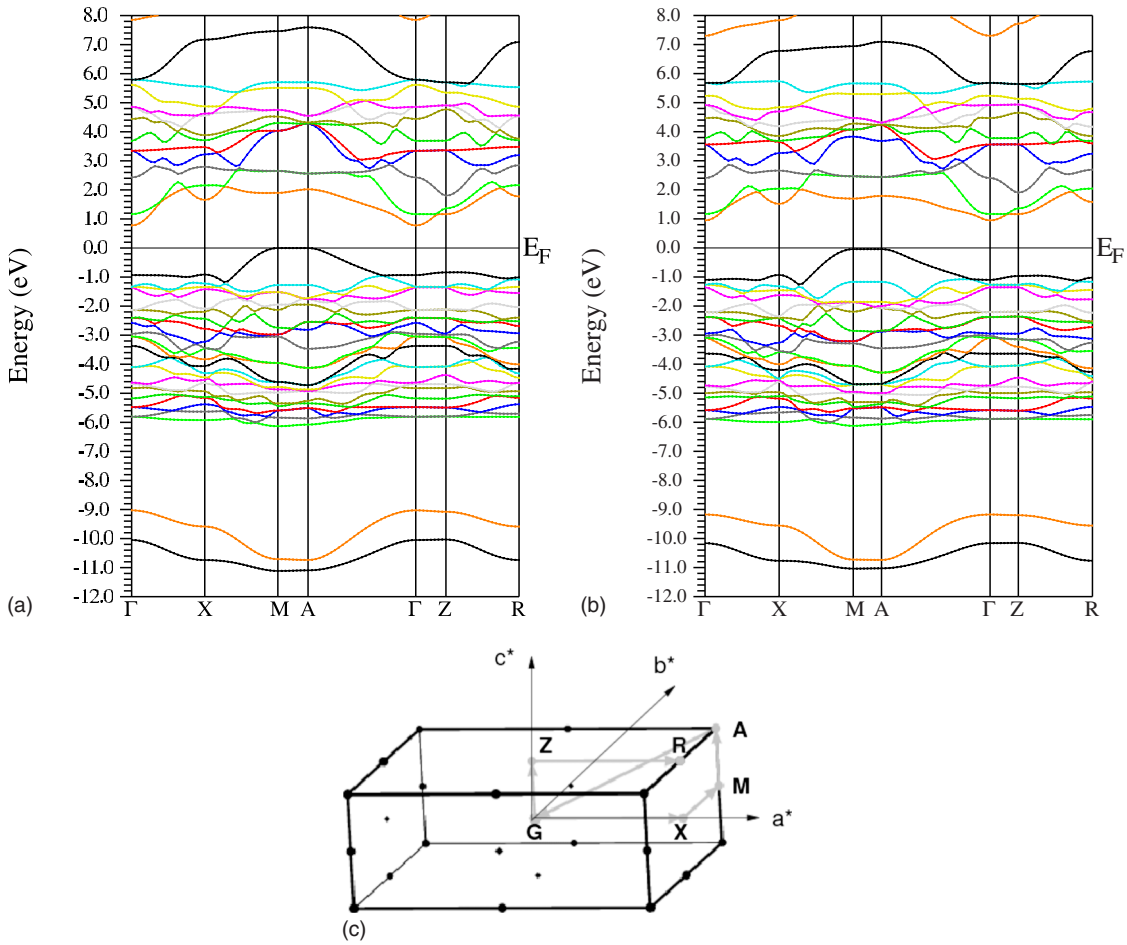

FIG. 3. (Color online) Band structures of the tetragonal Bi_2ZnTiO_6 with different tetragonalities of 1.211 (a) and 1.311 (b) along the high-symmetry directions in the Brillouin zone. (c) The Brillouin zone of the tetrahedral structure with high-symmetry points G (0,0,0), X (0.5,0,0), M (0.5,0.5,0), A (0.5,0.5,0.5), Z (0,0,0.5), and R (0.5,0,0.5). The symbols a*, b*, and c* denote the reciprocal vectors.

character from the bond length listed in Table III. The lowest part of band structure consists of Bi 6*s* derived peak, approximately located in the region from −11 to −9 eV below the Fermi energy. The valence band (VB) lying from −6 to −1 eV shows a substantial mixed character from all ions Bi, Zn, Ti, and O. The same is true for the conduction band in the region of 1–6 eV. For all BZT considered here, the top of VB at $M(A)$ point comes from occupied O 2*p* states, and the bottom of the conduction band at Γ point is composed of unoccupied Bi 6*p* states. An indirect band gap is thus formed between Γ-M points. As tetragonality increases from 1.211 to 1.311, the band gap changes from 0.8 to 1.0 eV. Since GGA usually underestimates the band gap, the experimental value should be larger than the theoretical one.

It is noted that the Bi–O bonding determines the electronic properties of BZT, which is similar to the situation in simple hypothetical $BiMO_3$ compounds.[12] In addition, the band structures of BZT show smaller energy dispersions than those in simple perovskite $BiMO_3$ compounds,[12] indicating a larger electronic localization effect in the former system. The band structures along both *M*-*A* and Γ-Z directions in the entire energy region considered are found to be extremely flat, indicating a remarkable strong bonding. This contributes to the short Ti/Zn–O bond length in the [001] direction (listed in Table III). The flat band structure along Γ-Z has also been reported in $Bi_4Ti_3O_{12}$.[32]

2. DOS

The calculated total DOS (TDOS) for BZT with tetragonalities of 1.211 and 1.311 are shown in Fig. 4. Fermi level is located at 0 eV. It is evident that there is no substantial difference in the shape of two BZTs, particularly in energy regions below 6 eV. It is observed that there are many hybridization peaks in the TDOS profile, indicating strong covalent bonding between ions, similar to the situation in ferroelectric

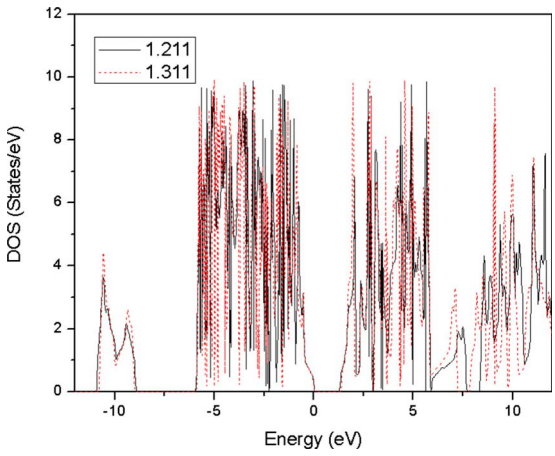

FIG. 4. (Color online) TDOSs for Bi_2ZnTiO_6 with tetragonalities of 1.211 and 1.311.

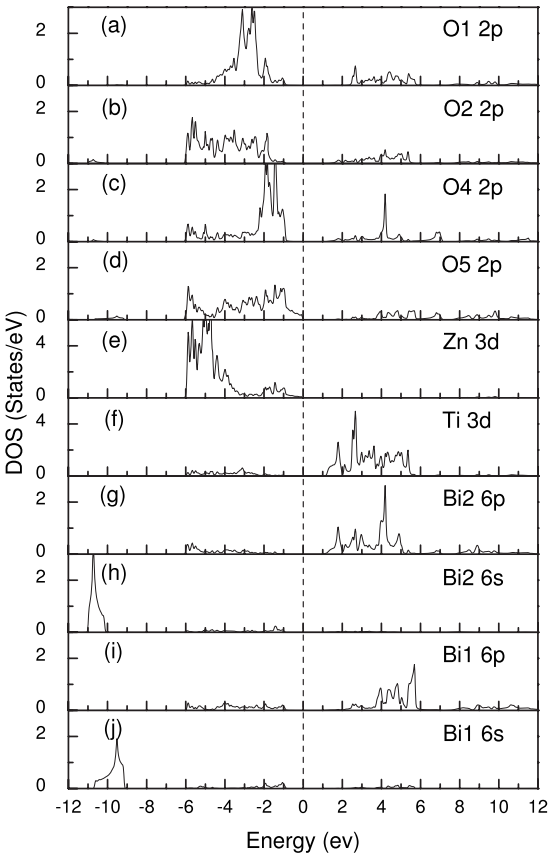

FIG. 5. PDOSs for Bi_2ZnTiO_6 with tetragonality of 1.311.

materials. The peak values of BZT with tetragonality of 1.311 is slightly larger than that with tetragonality of 1.211, suggesting a slightly stronger covalent bonding. The partial DOSs (PDOSs) with tetragonality of 1.311 are shown in Fig. 5. It can be seen that the VB originates predominantly from Zn 3*d* and O 2*p* states with some contributions from Bi 6*sp* and Ti 3*d*. It is noted that the role of Zn 3*s* can be ignored since it is very weak (figure not shown here). The conduction band mainly consists of Ti 3*d*, Bi 6*p*, and O 2*p* states. It is found that Zn ions contribute more to the VB, while Ti ions contribute more to the conduction band. In addition, the PDOSs of O atoms are different from each other, suggesting that their bonding environments are different (as later shown in Fig. 7 and 8). In Fig. 6, both O1 and O4 have a strong hybridization with Zn/Ti due to the existence of short Ti–O1/Zn–O4 bond length, while O2 and O5 do not have because of their large bond lengths with Zn/Ti ions.

Equal VB (or conduction band) peak values indicate obvious hybridizations of $B(\mathrm{Zn/Ti})-\mathrm{O}$ and $A(\mathrm{Bi})-\mathrm{O}$. Many sharp hybridization peaks are clearly shown in the PDOS profile in Fig. 6. This indicates very strong hybridizations between Bi 6*p* and O 2*p* orbitals as well as between $B(\mathrm{Zn,Ti})$ 3*d* and O 2*p* ones. Compared to the bonding situation in $Bi_4Ti_3O_{12}$ (Ref. 32) or simple hypothetical cubic perovskite $BiMO_3$ compounds,[12] the hybridization of Bi–O in BZT as well as Ti–O is stronger in conduction band, while the hybridization of Zn–O is stronger in VB. This suggests the covalent nature of the $B(\mathrm{Zn,Ti})-\mathrm{O}$ and Bi–O bondings, like covalent bonding of Ti–O and Pb–O in $PbTiO_3$. The covalent bonding means that the charge partially transfers

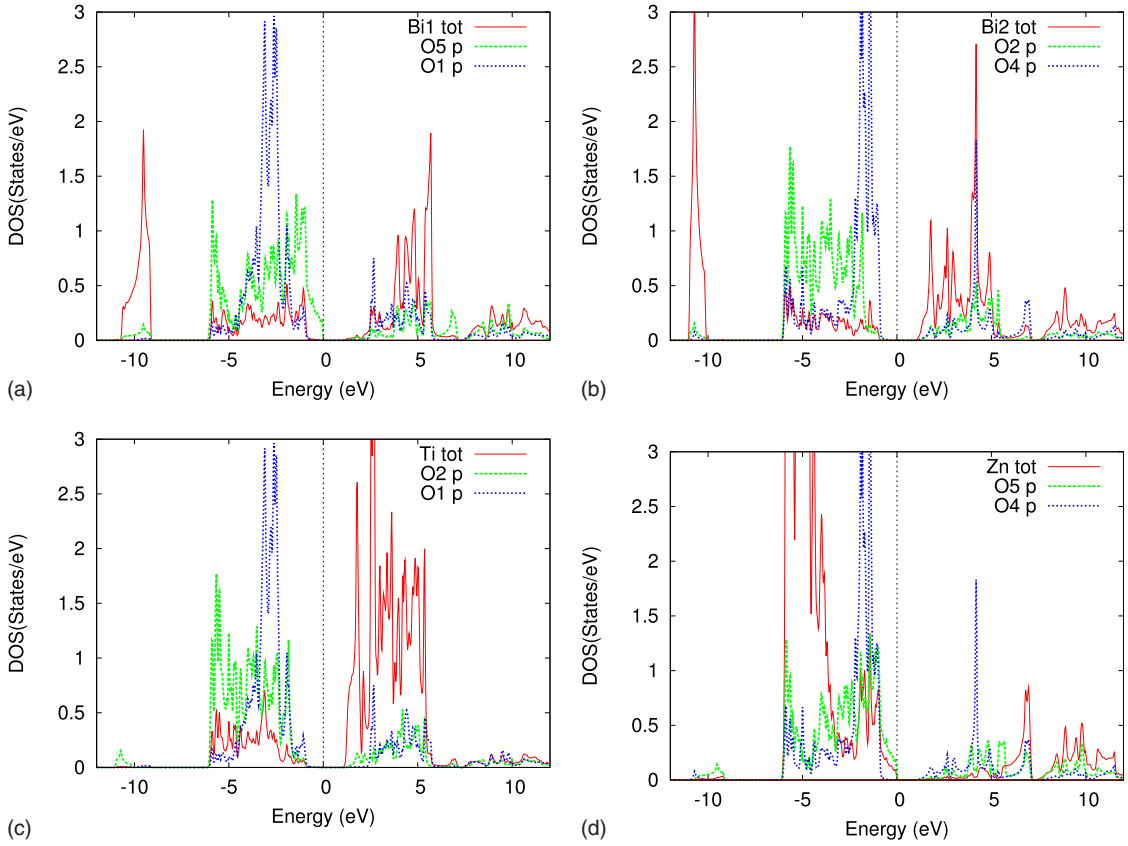

FIG. 6. (Color online) PDOSs for Bi_2ZnTiO_6 with tetragonality of 1.311.

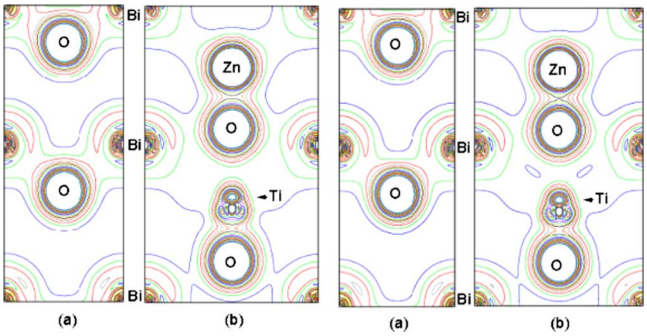

FIG. 7. (Color online) Charge density maps for (100) (a) and (110) (b) planes in BZT with tetragonalities of 1.211 (left panel) and 1.311 (right panel).

from one ion to the other and two ions share some electrons, i.e., the Bi–O covalent bonding should be a charge transfer between Bi and O ions, while $B(\mathrm{Zn},\mathrm{Ti})-\mathrm{O}$ bonding a charge transfer between *B*-site Zn, Ti and O ions. Therefore, there is a superinteraction between *A*-O-*B* ions through O ions, i.e., the electrons can transfer between all *A*, *B*, and O ions. Due to the fact that when the tetragonality increases all atoms exhibit a collective off-center displacement behavior in order to keep the bond length as unchanged as possible, the *B*-O (*B*-site ions and oxygen) hybridization therefore has a strong coupling with the *A*-O (*A*-site ions and oxygen) one through the superinteraction of *A*-O-*B* ions. So, the coupling strengthens *A*-O and/or *B*-O hybridization itself and it also favors the coupled structural distortions of *A*- and *B*-site ions, i.e., the energetically favorable off-center displacements, as mentioned previously. Similar coupling between *B*-O and *A*-O bonds has also been theoretically demonstrated in simple perovskite $BiMO_3$ compounds.[12] Recently, Grinberg *et al.*[23] suggested that Zn–O hybridization also favors the coupling between *A*- and *B*-site displacements in the BZT-$PbTiO_3$ solid-solution systems. In addition, it has been reported in $Bi_4Ti_3O_{12}$ compound that the hybridization of Ti–O in the perovskite layers is enhanced indirectly by the Bi–O hybridization, which is the origin of ferroelectricity.[32]

3. Charge density

The charge density maps for (100) and (110) planes in BZT with different tetragonality are illustrated in Figs. 7 and 8. It is observed that there is no obvious qualitative change in bonding nature. This is consistent with the slight change in bond length. In addition, the covalent interactions between Bi and O ions, which do not exist in simple cubic $BiMO_3$ compounds,[12] are strong and so are the Zn–O and Ti–O covalent bondings. For comparison, the charge density map of $PbTiO_3$, calculated using experimental structure data, is shown in Fig. 9. The results on PT agree well with that in Ref. 37. When Fig. 7 is compared with Fig. 9, it becomes evident that there is surprising similarity in the density map between BZT and PT. Therefore, a strong two-dimensional covalent bonding is also formed in BZT just like that in PT (Ref. 37) [three-dimensional view is shown in Fig. 2(e)]. Considering previous analysis, the two-dimensional covalent-bonding means that the electron transfer between cations Bi/Ti/Zn and anions O is very easy, and the coupling

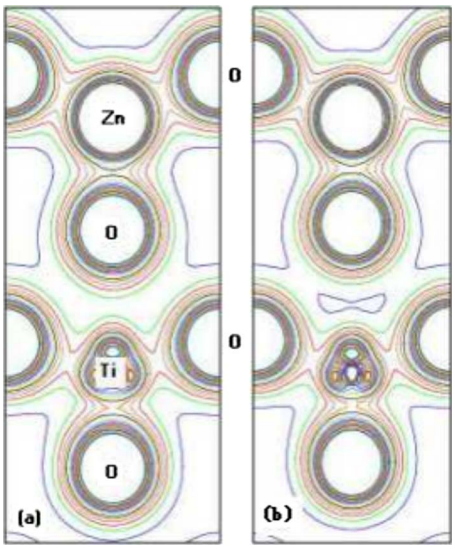

FIG. 8. (Color online) Charge density maps for (100) planes through Zn–O–Ti–O in BZT with different tetragonalities of 1.211 (a) and 1.311 (b).

between the bondings of Bi–O and Ti–O/Zn–O is strong. As tetragonality increases, the localization of electron only slightly increases, resulting two-dimensional character more observable. In addition, it can be seen clearly that Bi 6*s* lone pair has a lobe shape. Its role on structure distortion has been discussed in the $BiMO_3$ compound.[11]

C. The polarization of BZT and the role of Zn

Using Berry-phase method,[29,30] the spontaneous polarizations of BZTs with different tetragonality have been calculated and the results are listed in Table I. The Berry-phase polarization was calculated with the reference centrosymmetric structure, for which polarization was set zero. Here we only give the polarization with 100% displacements. Our calculations show that BZT has a polarization as high as 122 $\mu\mathrm{C}/\mathrm{cm}^2$, which is huge and attractive for potential applications. The huge polarization of BZT results from the large tetragonality c/a and the substantial internal atomic off-center displacements. The stability of huge tetragonality of BZT is discussed as follows. On one hand, the strong Bi–O hybridization in BZT results in a shorter Bi–O bond

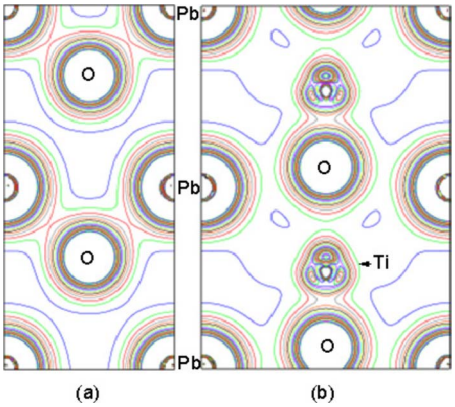

FIG. 9. (Color online) Charge density maps for (100) (a) and (110) planes (b) in $PbTiO_3$ with experimental tetragonal structure.

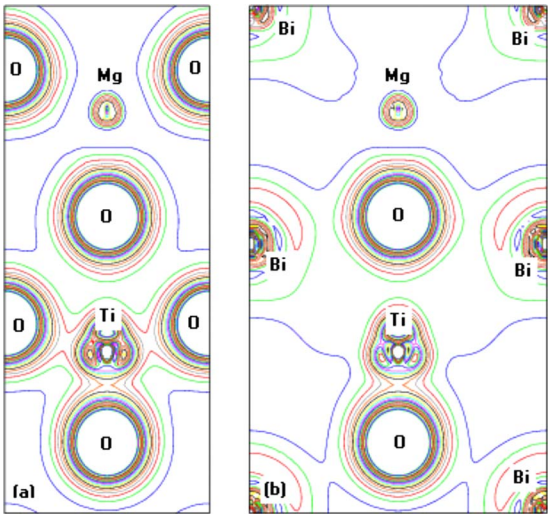

FIG. 10. (Color online) Charge density maps for (100) plane through Mg–O–Ti–O chain (a) and (110) plane (b) in Bi_2MgTiO_6 using the BZT structure with tetragonality of 1.311.

length and therefore a lattice constant (a=3.791 Å) smaller than that in a general perovskite structure (a=4.0 Å). Such a small lattice constant is helpful to keep the large tetragonality, similar to the constraint on films from substrates. On the other hand, the strong covalence of Zn–O/Ti–O chains along c direction, which induces the ferroelectric instability in ABO_3 perovskite compounds,[38,39] is also beneficial to the stabilization of large tetragonality.[40] Moreover, since the coupling between tetragonality and internal atomic off-center displacements is energetically favorable, the resulting large tetragonality in BZT is stable and has been experimentally confirmed.[20]

To reveal the role of Zn ions, we performed the charge density calculations on Bi_2MgTiO_6 (BMT), employing the BZT structure with the substitution of Zn by Mg and with a tetragonality of 1.311. The charge density maps in Fig. 10 show that the bonding of Mg–O has an ionic nature, which is substantially different from the Zn–O bonding in BZT. It is well known that covalent bond is essential for ferroelectricity.[40] Therefore, the ionic bonding of Mg–O makes Mg and O ions lose the driving force of off-center displacement along the [001] direction and results in the absence of ferroelectricity in BMT.

IV. CONCLUSIONS

In summary, the structural and electronic properties of Bi_2ZnTiO_6 have been calculated using the supercell method. The theoretical structure we obtained confirms the extra large tetragonality observed by experiment. The materials exhibit a semiconductor behavior with an indirect band gap between the occupied O 2p and unoccupied Bi 6p states. There are strong hybridization effects between Bi–O ions as well as Ti–O and Zn–O ones. The covalent resulting bondings strengthen each other and favor the coupling between the tetragonal distortion of unit cell and off-center displacements of A- and B-site cations due to the presence of Zn. This stabilizes BZT with a large tetragonality. Our study suggests that the coupling between the A- and B-site ionic displacements should be examined in the first instance in the search of B-site complex $BiMM'O_3$ compounds with large tetragonality or in the search of Bi-based multiferroics with a strong coupling between ferroelectric and magnetic orders. Finally, we propose that Bi_2ZnTiO_6 doped with a magnetic atom may be a promising multiferroic with strong ferromagnetic coupling, if the strong coupling of A-O-B is preserved.

ACKNOWLEDGMENTS

This work was supported by the National Science Foundation of China (Grant Nos. 10572155, 10172030, and 50232030) and was partially supported by grants from the Research Grants Council of the Hong Kong Special Administrative Region (Project No. PolyU 5171/07E), and the Hong Kong Polytechnic University (Project No. G-YF71).

[1] J. Wang, J. B. Neaton, H. Zheng, V. Nagarajan, S. B. Ogale, B. Liu, D. Viehland, V. Vaithyanathan, D. G. Schlom, U. V. Waghmare, N. A. Spaldin, K. M. Rabe, M. Wuttig, and R. Ramesh, Science **299**, 1719 (2003).
[2] A. K. Tagantsev, I. Stolichnov, N. Setter, J. S. Cross, and M. Tsukada, Phys. Rev. B **66**, 214109 (2002).
[3] T. Kimura, S. Kawamoto, I. Yamada, M. Azuma, M. Takano, and Y. Tokura, Phys. Rev. B **67**, 180401 (2003).
[4] R. Eitel, C. A. Randall, T. R. Shrout, P. Rehrig, W. Hackenberger, and S.-E. Park, Jpn. J. Appl. Phys., Part 1 **40**, 5999 (2001).
[5] R. Eitel, C. A. Randall, T. R. Shrout, and S. E. Park, Jpn. J. Appl. Phys., Part 1 **41**, 2099 (2002).
[6] S. J. Zhang, C. A. Randall, and T. R. Shrout, Appl. Phys. Lett. **83**, 3150 (2003).
[7] J. R. Cheng, W. Y. Zhu, N. Li, and L. E. Cross, Mater. Lett. **57**, 2090 (2003).
[8] R. R. Duan, R. F. Speyer, E. Alberta, and T. R. Shrout, J. Mater. Res. **19**, 2185 (2004).
[9] Y. Inaguma, A. Miyaguchi, M. Yoshida, T. Katsumata, Y. Shimojo, R. P. Wang, and T. Sekiya, J. Appl. Phys. **95**, 231 (2004).
[10] S. J. Zhang, R. Xia, C. A. Randall, T. R. Shrout, R. R. Duan, and R. F. Speyer, J. Mater. Res. **20**, 2067 (2005).
[11] P. Baettig, C. F. Schelle, R. LeSar, U. V. Waghmare, and N. A. Spaldin, Chem. Mater. **17**, 1376 (2005).
[12] H. Wang, B. Wang, Q. K. Li, Z. Y. Zhu, R. Wang, and C. H. Woo, Phys. Rev. B **75**, 245209 (2007).
[13] A. A. Belik, M. Takano, M. V. Boguslavsky, S. Y. Stefanovich, and B. I. Lazoryak, Chem. Mater. **18**, 133 (2006).
[14] A. A. Belik, S. Iikubo, K. Kodama, N. Igawa, S. Shamoto, M. Maie, T. Nagai, Y. Matsui, S. Y. Stefanovich, B. I. Lazoryak, and E. Takayama-Muromachi, J. Am. Chem. Soc. **128**, 706 (2006).
[15] A. A. Belik, S. Iikubo, K. Kodama, N. Igawa, S. Shamoto, S. Niitaka, M. Azuma, Y. Shimakawa, M. Takano, F. Izumi, and E. Takayama-Muromachi, Chem. Mater. **18**, 798 (2006).
[16] A. A. Belik, S. Y. Stefanovich, B. I. Lazoryak, and E. Takayama-Muromachi, Chem. Mater. **18**, 1964 (2006).
[17] Y. Inaguma and T. Katsumata, Ferroelectrics **286**, 111 (2003).
[18] M. Azuma, K. Takata, T. Saito, S. Ishiwata, Y. Shimakawa, and M. Takano, J. Am. Chem. Soc. **127**, 8889 (2005).
[19] D. D. Khalyavin, A. N. Salak, N. P. Vyshatko, A. B. Lopes, N. M. Olekhnovich, and A. V. Pushkarev Maroz, II, and Y. V. Radyush, Chem. Mater. **18**, 5104 (2006).
[20] M. R. Suchomel, A. M. Fogg, M. Allix, H. J. Niu, J. B. Claridge, and M. J. Rosseinsky, Chem. Mater. **18**, 4987 (2006); **18**, 5810 (2006).
[21] J. Chen, P. Hu, X. Sun, C. Sun, and X. Xing, Appl. Phys. Lett. **91**, 171907 (2007).
[22] Y. K. Kim, S. S. Kim, H. Shin, and S. Baik, Appl. Phys. Lett. **84**, 5085 (2004).
[23] I. Grinberg, M. R. Suchomel, W. Dmowski, S. E. Mason, H. Wu, P. K. Davies, and A. M. Rappe, Phys. Rev. Lett. **98**, 107601 (2007).
[24] P. Blaha, K. Schwarz, G. Madsen, D. Kvasnicka, and J. Luitz, WIEN2k, an augmented plane wave plus local orbitals program for calculating crystal properties, Vienna University of Technology, Vienna, 2001.
[25] J. P. Perdew, K. Burke, and M. Ernzerhof, Phys. Rev. Lett. **77**, 3865 (1996).

[26]P. E. Blochl, O. Jepsen, and O. K. Andersen, Phys. Rev. B **49**, 16223 (1994).
[27]G. Kresse and J. Furthmüller, Comput. Mater. Sci. **6**, 15 (1996); Phys. Rev. B **54**, 11169 (1996).
[28]P. E. Blöchl, Phys. Rev. B **50**, 17953 (1994); G. Kresse and D. Joubert, *ibid.* **59**, 1758 (1999).
[29]R. D. King-Smith and D. Vanderbilt, Phys. Rev. B **47**, 1651 (1993); R. Resta, Rev. Mod. Phys. **66**, 899 (1994).
[30]D. Vanderbilt and R. D. King-Smith, Phys. Rev. B **48**, 4442 (1993).
[31]C. Kittel, *Introduction to Solid State Physics*, 6th ed. (McGraw-Hill, New York, 1986), p. 76.
[32]M. Q. Cai, Z. Yin, M. S. Zhang, and Y. Z. Li, Chem. Phys. Lett. **399**, 89 (2004).
[33]Z. Wu and R. E. Cohen, Phys. Rev. Lett. **95**, 037601 (2005).
[34]S. Tinte, K. M. Rabe, and D. Vanderbilt, Phys. Rev. B **68**, 144105 (2003).
[35]H. Huang, C. Q. Sun, Z. Tianshu, and P. Hing, Phys. Rev. B **63**, 184112 (2001).
[36]H. Huang, C. Q. Sun, and P. Hing, J. Phys.: Condens. Matter **12**, L127 (2000).
[37]Y. Kuroiwa, S. Aoyagi, and A. Sawada, Phys. Rev. Lett. **87**, 217601 (2001).
[38]R. Yu and H. Krakauer, Phys. Rev. Lett. **74**, 4067 (1995).
[39]Y. X. Wang, C. L. Wang, M. L. Zhao, and J. L. Zhang, Chin. Phys. Lett. **22**, 469 (2005).
[40]R. E. Cohen, Nature (London) **358**, 136 (1992).